GEOPHYSICS, VOL. 65, NO. 4 (JULY–AUGUST 2000); P. 1070–1079, 10 FIGS.

CSAMT exploration at Sellafield: Characterization of a potential radioactive waste disposal site

Martyn J. Unsworth*, Xinyou Lu*, and M. Don Watts‡

ABSTRACT

The long term disposal of radioactive waste in an underground repository requires the detailed geological evaluation of a potential site. Owing to their inherent sensitivity to the presence of fluids in rocks, electromagnetic (EM) methods have an important role in this assessment. Controlled-source EM techniques are especially useful in strong anthropogenic noise environments such as industrial locations. However the complexity of modeling and inversion can limit the quantitative interpretation of controlled-source EM data.

A potential radioactive waste disposal site at Sellafield in Great Britain has been investigated using a variety of EM exploration techniques. Controlled-source audio-frequency magnetotelluric (CSAMT) data have given the best subsurface information in an environment that has a high level of cultural noise. One-dimensional inversions of the Sellafield CSAMT data were found to be inadequate; 2.5-D forward modeling and inversion were used to interpret the data. The resulting resistivity models show good agreement with well log data collected at the site. These resistivity models show the presence of a large zone of hypersaline groundwater extending 1 km inland towards the potential repository and indicate the effect of faults on the hydrogeology.

INTRODUCTION

The long-term disposal of radioactive waste is a serious problem facing many countries with nuclear power programs. To determine a suitable underground location requires an extensive characterization of a potential site. A key characteristic to be determined is the present groundwater system and the inference of what changes might occur during the lifetime of the facility, which may be more than 100,000 years. Subsurface electrical resistivity is inherently related to the rock porosity and the groundwater chemistry. Thus remote sensing of the subsurface electrical resistivity with electrical and electromagnetic (EM) exploration techniques is an important part of site characterization. Previous EM investigations at potential repository or research facilities include studies at the Carlsbad Waste Isolation Pilot Plant (WIPP) in New Mexico (Bartel, 1990), the high-level waste site beneath Yucca Mountain (Majer et al., 1996), and a Canadian underground laboratory in Manitoba (Soonawala et al., 1990). A pilot study was also conducted at a potential intermediate-level waste repository near Sellafield in the United Kingdom (Watts, 1994).

Studies for a deep (>500 m) repository require exploration to a depth of more than 1 km, and EM exploration techniques with good depth penetration such as magnetotellurics (MT) are required. However intense cultural noise at such sites can obscure the natural EM fields used by MT. Controlled-source audio-frequency magnetotellurics (CSAMT) is a frequency-domain EM method that uses a grounded dipole or horizontal loop to generate repetitive artificial EM signals. CSAMT has been applied to mineral exploration, geothermal studies, hydrocarbon exploration, and groundwater studies (Zonge and Hughes, 1991). Controlled-source methods have the advantage that data can be collected in areas of high cultural noise, where natural source MT singals would not be detectable. Even in a quiet environment, artificial repeatable source fields can speed up the acquisition of data in the audio-frequency range where natural fields have low amplitude.

Far from the transmitter, the electromagnetic fields are planar, and CSAMT data can be interpreted using conventional approaches developed for MT data. However, to interpret data close to the transmitter, the analysis must account for the 3-D nature of the electromagnetic fields generated by the transmitter. This important difference between MT and CSAMT data is illustrated in Figure 1, which shows a typical sounding over a three-layer earth. At high frequencies, the CSAMT and MT responses are identical because the receiver lies in the far field

Presented at the 67th Annual Meeting, Society of Exploration Geophysicists. Manuscript received by the Editor December 23, 1998; revised manuscript received January 4, 2000.
*University of Washington, Geophysics Program, ATG-220, Box 351650, Seattle, Washington 98195-1650. E-mail: unsworth@geophys.washington.edu.
‡Geosystem, Viale Abruzzi, 17, Milan, Italy. E-mail: dwatts@geosystem.net.

of the transmitter. Electromagnetic fields travel from transmitter to receiver through the air and then diffuse vertically into the earth. At low frequencies in the near field, the apparent resistivities are anomalously high while the phase between the electric and magnetic fields is close to 0°, and electromagnetic fields travel horizontally through the earth to the receiver. At intermediate frequencies, the electromagnetic signal diffusing to the receiver through the earth becomes comparable in strength to that propagating through the air, resulting in a notch with very low apparent resistivity.

To interpret near- and intermediate-field CSAMT data correctly requires that the 3-D nature of the transmitter fields are adequately modeled. Attempts have been made to correct transition zone and near-field CSAMT data to the equivalent plane-wave MT data (e.g., Bartel and Jacobson, 1987). However, this technique lacks a physical basis and can introduce artifacts into the corrected data. If the EM response indicates the earth is demonstrably 1-D, the simulation is straight forward (Boerner and West, 1984; Boerner et al., 1993). If the subsurface displays higher dimensionality, then an analysis that permits a 2-D or 3-D resistivity model of the earth may be needed. In this paper, we describe the application of 2.5-D inversion and modeling to CSAMT data collected at a potential radioactive waste repository near Sellafield in northwest England.

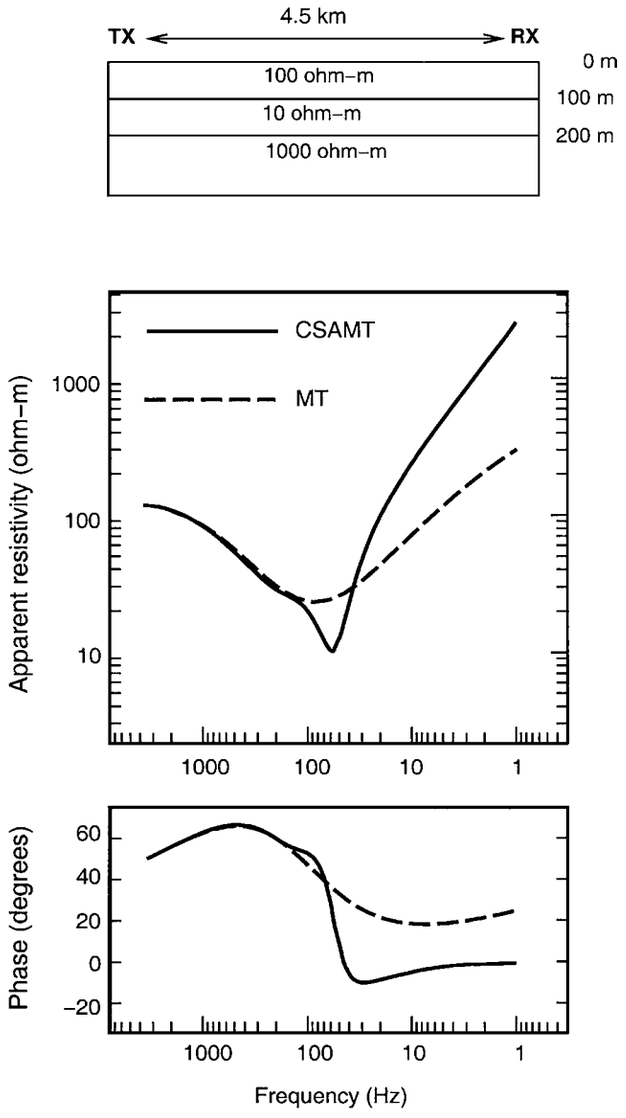

FIG. 1. Apparent resistivity and phase computed for MT and CSAMT soundings over a layered earth. Transmitter-receiver geometry for the CSAMT data is equivalent to TE mode.

PREVIOUS GEOLOGICAL AND GEOPHYSICAL STUDIES OF THE SELLAFIELD AREA

NIREX, the United Kingdom company responsible for the disposal of intermediate and some low-level radioactive waste, evaluated a site near Sellafield in northwest England as a potential underground repository. This investigation drew on a wide range of geological, geophysical, and hydrogeological data (Chaplow, 1996). In the Sellafield area (Figure 2), geological mapping and extensive deep drilling has shown that there is an upper sequence of sedimentary rocks that thicken to the west into the offshore basin. The dominant units are the St. Bees and Calder Sandstone formations, both Permo-Triassic in age. These units overly basement of the Ordovician Borrowdale Volcanic Group (BVG) that crops out in the eastern part of the survey area. The potential repository lies within the BVG at a depth of 600–700 m below sea level about 3 km inland from the Irish Sea. Seismic reflection surveys have indicated that major faults run parallel to the coast, but other faults lie normal to the coast. This geological framework provided a major control on the hydrogeology (Michie, 1996). Groundwater in the near surface aquifer is fresh to depths of 200–500 m. Close to the Irish Sea, the groundwater at depth in the deep boreholes was found to be highly saline, with brines several times the salinity of seawater. Inland at the potential repository level, the salinity was about 0.7 times that of seawater (Bath et al., 1996).

As part of the site characterization activities, electromagnetic surveys were performed in 1995 by Geosystem. Time-domain EM, MT, and CSAMT surveys were carried out in the area surrounding the potential repository. The goal of these surveys was to map subsurface resistivity structure with the emphasis on characterizing hydrogeology in areas without deep borehole data. It was anticipated that information about rock properties obtained from deep drilling would allow resistivity data to be interpreted in terms of salinity. Without any other information, EM methods cannot separate the rock porosity and fluid salinity. However, at Sellafield, a detailed data base of the porosity of individual rock units was available from wireline logs and core samples. Thus resistivity measurements of the subsurface can be used to determine the resistivity of the pore fluid, and hence its salinity through measured or empirical relationships such as Archie's Law.

MT data were recorded at 27 sites and were generally of low quality since the relatively weak natural EM fields were contaminated by electrical noise from the nuclear power plants and other facilities at the Sellafield Works, numerous powerlines, and cathodically protected pipelines. Time-domain EM data were collected using a Sirotem-2 system in the central loop configuration with 100×100 m loops. These data were noise free to ~5 ms but at later times, coupling with local grounded metallic structures was found to contaminate the soundings. Thus their effective penetration was limited to less than 250 m.

SELLAFIELD CSAMT DATA ACQUISITION, MODELING, AND INVERSION

Artificial EM fields were generated with a Zonge GGT-30 transmitter that was placed at two locations (Figure 2). The first transmitter location was at Nethertown, about 14 km northwest of Sellafield and located perpendicular to the coast. This transmitter produced high-quality data, but they were not interpretable with a 2-D model owing to the interaction of the transmitter with the conductive seawater that produced complex effects in the data. A second transmitter location was chosen inland at Bleng Fell (Figure 2); signals from this site were generally stronger because of the more resistive rocks that lay between the transmitter and the Sellafield site, dominantly the BVG. In contrast, the Nethertown transmitter site lay on the sedimentary sequence and close to the Irish Sea, giving a higher attenuation of EM signals on the path from transmitter to receiver. However, this enhancement in signal-to-noise ratio from the Bleng Fell site in the resistive BVG also resulted in near-field and transition-zone data in the region of investigation.

CSAMT data were recorded at 245 locations using a 10-channel EMI MT-1 system. At each location data were recorded from 4096 to 1 Hz and processed to give estimates of apparent resistivity and phase. Many sites were unusable, either due to active noise from powerlines or pipelines, or because of distortion of EM fields by local conductors. The highest quality data were identified and grouped for analysis and interpretation into four profiles running perpendicular to the coast. Apparent resistivities were approximately corrected for static shift using the time-domain EM data previously described. Figure 3 shows CSAMT data at two typical sites on line 1. At site 18, the most distant from the transmitter, the high apparent resistivities and low phases that characterize the near field are only present below 3 Hz. In contrast, at site 9, the effect of the transmitter is obvious below 100 Hz. Figure 4a shows the CSAMT data collected along line 1 in pseudosection format. The orientation of the transmitter was parallel to strike, as were the electric fields used to define apparent resistivity, so this data is analogous to the TE mode in conventional MT. Because the skin depth effect causes the lower frequencies to penetrate further into the earth, the low-frequency apparent resistivities are plotted at the bottom of each pseudosection, giving an impression of how resistivity varies with depth. As in Figure 3, note the high apparent resistivities that move to lower frequencies as the transmitter-receiver offset increases. This is partly due to the effect of the transmitter as shown in Figure 1 (Zonge and Hughes, 1991). However, the local geology described by Michie (1996) mirrors this effect with a thickening sequence of relatively conductive sedimentary rocks to the southwest overlying the more resistive BVG, which crops out in the northeast. To obtain a realistic picture of the groundwater salinity, it is important to determine how much of the high apparent resistivity derives from the geoelectric structure and how much is due to the near field of the transmitter.

1-D CSAMT inversion

The CSAMT data were initially fit to a 1-D resistivity model using an inversion based on the forward calculation of Boerner and West (1984). The results of two typical inversions are shown in Figure 5 and compared with blocked well log data from

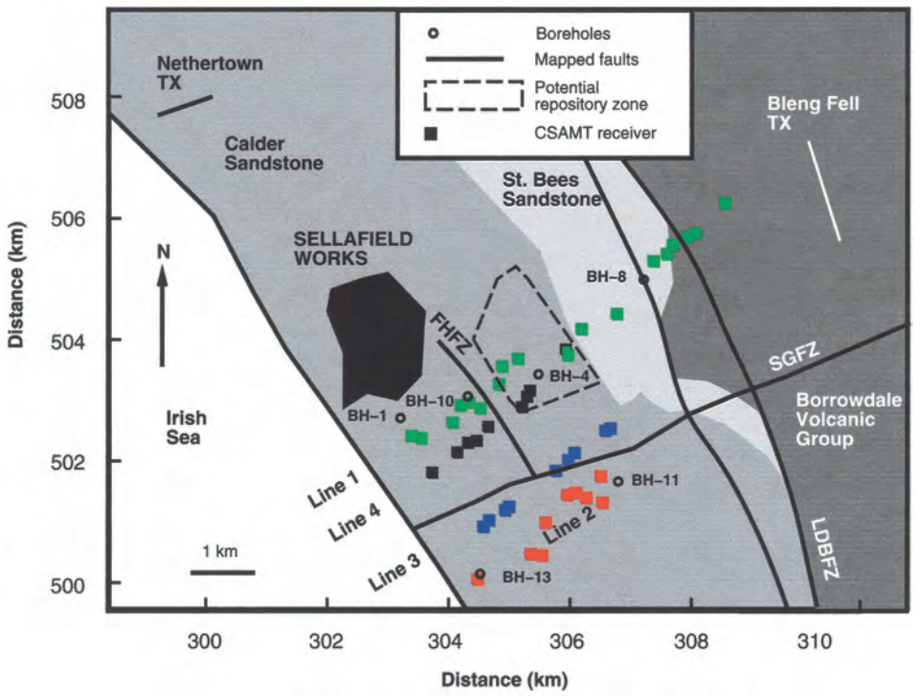

FIG. 2. Map of the survey area showing simplified geology and the layout of the CSAMT survey. LDBFZ = Lake District Boundary Fault Zone, SGFZ = Seascale Gosforth Fault Zone, FHFZ = Fleming Hall Fault Zone, TX = transmitter location. North-south and east-west distances are United Kingdom National Grid coordinates.

nearby boreholes collected with a Schlumberger dual laterolog tool. When comparing resistivity data from wireline logging and surface exploration techniques, the differing resolution of each method must be considered. Wireline logging samples a small volume and can detect scale features close to the well. In contrast, surface exploration uses long wavelength signals that will average the resistivity with length scales comparable to the depth of exploration. Thus, the CSAMT inversion model will generally be smoother than the well log data. At a site on line 1 that was adjacent to borehole BH-1, the 1-D CSAMT inversion images a conductor at approximately the correct depth, but significantly underestimates the conductance. Further inland at BH-4, the 1-D inversion correctly images the top of the resistive BVG at a depth of 400 m. However at depths below 1000 m, the 1-D inversion introduces a conductor that is inconsistent with the well log data and regional geology. This false conductor was observed in the 1-D CSAMT inversions at a number of sites and may be due to CSAMT data detecting the conductive zone to the southweast, or possibly the Irish Sea. Since a 1-D inversion cannot allow for lateral variations, the only way the data can be fit is by placing the conductor beneath the site.

2.5-D forward modeling

The raw CSAMT data (Figure 4a) and the 1-D inversions indicate rapid lateral variations in resistivity beneath line 1. To examine the validity of the 1-D analysis, it was decided that using an extended 2-D earth model was required. To model the interaction of 3-D EM fields with a 2-D earth, the 2.5-D finite element code developed for ocean floor exploration by Unsworth et al. (1993) was adapted for onshore use. The data were analyzed using a trial-and-error approach that sought to match the calculated CSAMT response of a given model with the field data. This required that a geologic strike direction be chosen. The local geology (Figure 2) and orthogonality considerations indicated that a geoelectric strike direction parallel to the Bleng Fell transmitter was appropriate. The most satisfactory resistivity model for line 1 is shown in Figure 4b, and the response of the model is shown in Figure 4c. This fits the field data well as shown by comparison with Figure 4b. Numerically this model fits the data with a root-mean-square (rms) misfit of 2.8 and standard errors of 10%. A statistically acceptable fit would have an rms misfit of unity with each datum fit to within one standard error. Small static shift coefficients were needed to fit the apparent resistivity data at a number of sites. The Irish Sea is shallow at Sellafield (less than 50 m), but is still a significant conductor, so it was included in the 2-D resistivity model.

2.5-D CSAMT inversion

The iterative forward modeling described above is a good way to understand the sensitivity of features in the model to the field data. However, the CSAMT inverse problem is nonunique, and extra conditions are often applied to find a single solution. A common procedure in EM geophysics is to choose the smoothest model from the set of models that fit the data. This smoothing removes features not required by the data, and reflects the diffusive nature of low-frequency EM field field propagation in the earth. To implement this style

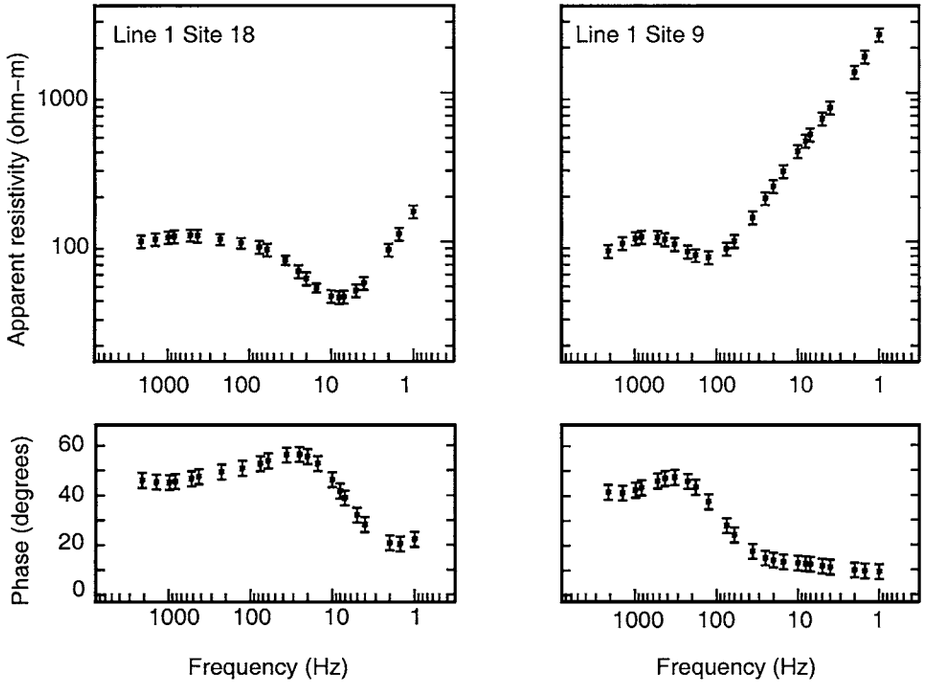

FIG. 3. CSAMT data at two locations on line 1. The rise in apparent resistivity at low frequency at site 9 is characteristic of the transmitter effect. Error bars on field data were very small, typically less than 1% in apparent resistivity and 1° in phase. Error bars shown are those used in modeling and inversion, and represent 10% in apparent resistivity and 3° in phase.

of inversion, the forward modeling described above was combined with the rapid relaxation inversion of Smith and Booker (1991) as described by Lu et al. (1999). The data for line 1 were then inverted; the resulting model is shown in Figure 6a. This contains essentially the same resistivity features as that obtained from forward modeling (Figure 4b) but lacks the sharp boundaries. This model fits the data with an rms misfit of 1.78, implying a slightly better fit to the measured data than the forward model in Figure 4b. The fit at two sites is shown as a function of frequency in Figure 7. Data on three additional profiles to the south were also inverted. On each of these profiles, the data is reproduced well by the model response, except at the eastern (right) end of the lines where apparent resistivity and phase are inconsistent, suggesting a minor 3-D effect. All four profiles image the conductive layer in the upper part of the western end of the profile, and this appears to extend further east on the southern most lines. Note also that the conductance of this layer increases to the south. Line 1 images resistive basement at a depth of 500 m beneath the eastern portion of the line, but is poorly imaged on lines 2–4 owing to their more restricted spatial coverage.

The resistivity models obtained by 2.5-D inversion were compared to well log resistivity data (Figures 8a and 9). At sites near the coast where the conductive layer is observed (BH-1 and BH-13), the inversion produces an estimate of conductivity that is more consistent with borehole logging than that derived from the 1-D CSAMT inversion (Figure 5). Further inland at BH-4, the Borrowdale volcanic unit lies at a depth of 400 m, as

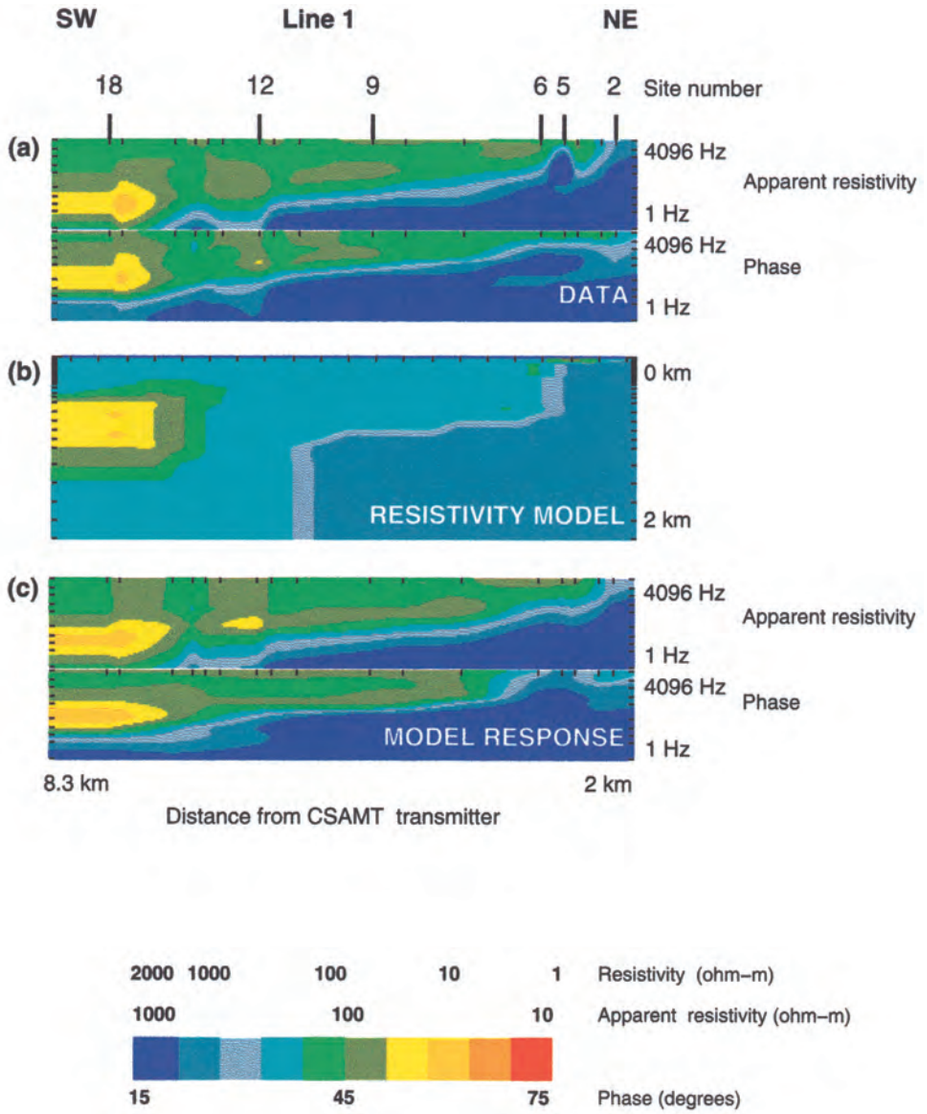

FIG. 4. (a) Data pseudosections for line 1 CSAMT data at Sellafield generated by the Bleng Fell transmitter. Geometry is such that this data is TE mode. Data were measured at sites denoted by tick marks on the horizontal axis. Frequencies used in the inversion and modeling are indicated by tick marks on the vertical axis. (b) Best-fitting resistivity model from forward modeling. Tick marks on the vertical scale denote the locations of nodes in the finite element mesh. (c) TE mode CSAMT response of model.

shown by the sharp rise in resistivity at this depth (Figure 5). At this location, the 2.5-D CSAMT inversion images a thin conductive layer from 200 to 400 m depth, in addition to the resistive basement. Note that the smoothed 2-D CSAMT inversion does not image a sharp change in resistivity. Nevertheless, the rapid rise in resistivity between 400 and 800 m depth indicates a major change of subsurface resistivity. The 2.5-D inversion does not produce a false conductor below 1000 m as was the case with the 1-D CSAMT inversion (Figure 5). At BH-10, the disagreement between the model and well log could be due to rapid lateral changes in resistivity within the Fleming Hall Fault Zone (FHFZ) not being represented in the CSAMT data. Further inland at BH-8 where the BVG is shallower, there is good agreement between well log and inversion model to a depth of 500 m (Figure 8a), but below this depth there is some disagreement.

INTERPRETATION OF RESISTIVITY MODELS

The electrical resistivity models of for line 1 (Figures 4b and 6a) show three distinct zones: (1) A low resistivity zone (<20 ohm-m) beneath the coast and extending ~1 km inland, (2) intermediate resistivities (20–200 ohm-m) in a surface layer that deepens to the west, and (3) a resistive (>200 ohm-m) zone underlying both (1) and (2). These three zones are closely related to the three zones of groundwater flow shown in the schematic model of Chaplow (1996) and summarized in Figure 8c.

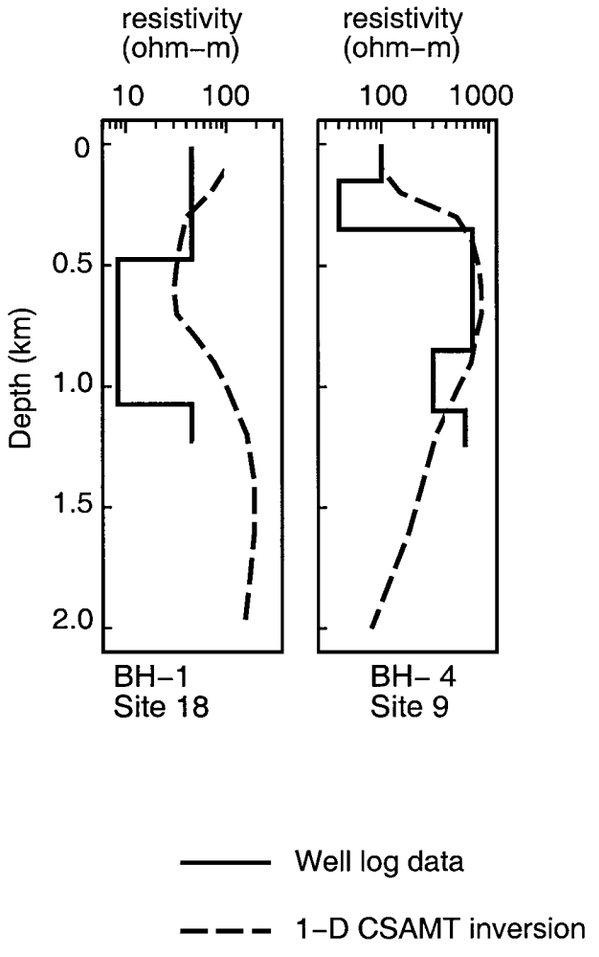

FIG. 5. Comparison of 1-D CSAMT inversions with resistivity data from well logs at BH-4 and BH-1. Data were collected using the Bleng Fell transmitter. The well logs have been composited by the calculation of accumulated conductance using the procedure of Strack (1992).

Coastal conductor

In this region there is good agreement between electrical resistivities derived from CSAMT inversion and well-dog data. Salinity measurements in BH-1 and BH-13 have shown that this conductor is due to a zone of hypersaline brines (Bath et al., 1996) whose chemistry indicates that they originate in the dissolution of Permo-Triassic evaporites. The brines are present in both the sedimentary rocks and the BVG, and constitute the Irish Sea Basin groundwater regime of Chaplow (1996). The principal sedimentary unit permeated by the brines is the St. Bees Sandstone, and in this unit well log data shows that resistivity is primarily dependent on pore-fluid salinity (implying a more or less constant porosity). Figure 10a illustrates that a resistivity of 10 ohm-m corresponds to a salinity of ~100 000 mg/liter Cl, in good agreement with salinity measured in the boreholes. In the zone where the hypersaline fluids saturate the BVG, resistivities are around 30 ohm-m, corresponding to a salinity of ~100 000 mg/liter Cl (Figure 10b). The eastern limit of the hypersaline zone as identified on the CSAMT model appears to correlate with Fault 17 identified by seismic reflection studies at Sellafield and shown in Figure 8a. While faults can act as flow conduits, they can also act as flow barriers. Thus, the eastern extent of the zone of hypersaline groundwater may be partially controlled by faulting. To the west, the hypersaline zone extends an undetermined distance beneath the Irish Sea. The brine zone is not entirely homogeneous. To the east of the ~100 000 mg/liter Cl region is a more resistive but still saline zone. This region represents a transition zone between the brines and less saline groundwater to the east. In this transition zone, resistivities in the Permo-Triassic sequence are in the range 20 to 100 ohm-m, and resistivities in the BVG are in the range 100 to 300 ohm-m. On line 1, the transition zone lies to the west of BH-10. These resistivities imply a salinity of ~10 000 mg/liter Cl. Note that the eastern boundary of the transition zone appears to correlate with the FHFZ. The location of the zone of hypersaline groundwater determined from borehole observations agrees well with the location mapped by the 2-D interpretation of the CSAMT data. The highly saline zone has a variable but gradually increasing conductance to the southeast. The increasing conductance may simply be due to the increased thickness of the Permian-Triassic sedimentary sequence beneath line 2. Note that line 2 lies south of the Seascale-Gosforth Fault Zone, which has a deeper sedimentary section on its southern side. The relatively slow variation of resistivity structure along strike further justifies the use of a 2-D resistivity model.

Shallow sedimentary layers

To the east of the transition zone, resistivities are higher in the sedimentary sequence. Borehole data indicates that the groundwater is fresh and the base of the low resistivity zone

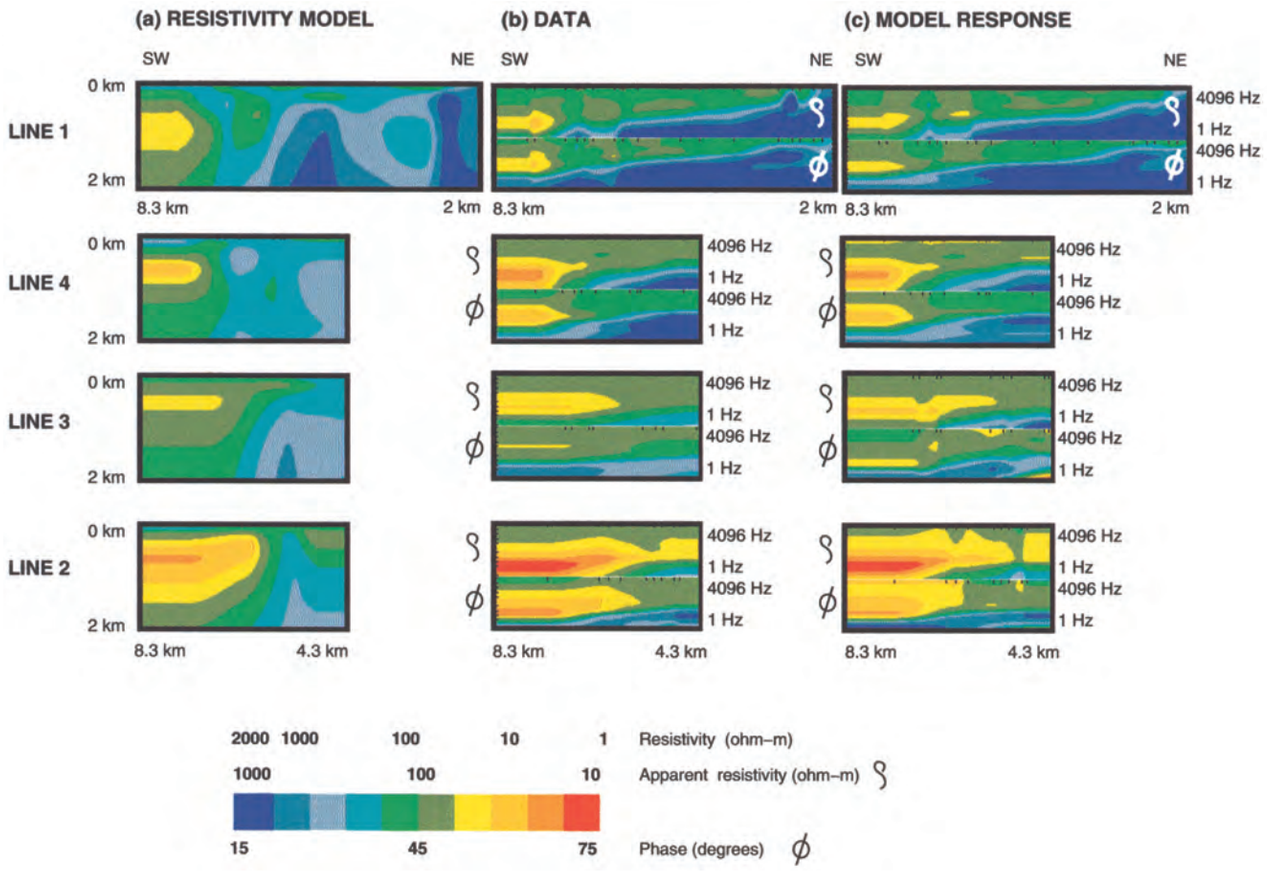

FIG. 6. (a) Resistivity models derived by 2-D inversion of TE mode CSAMT data. All models have vertical exaggeration of 1:1. (b) Observed data pseudosections for four lines of TE mode CSAMT data at Sellafield. Horizontal tick marks denote CSAMT receiver locations. (c) Computed CSAMT responses of best-fitting models shown in (a). Line 1 rms misfit = 1.6, line 4 rms misfit = 1.5, line 3 rms misfit = 2.2, line 2 rms misfit = 2.4.

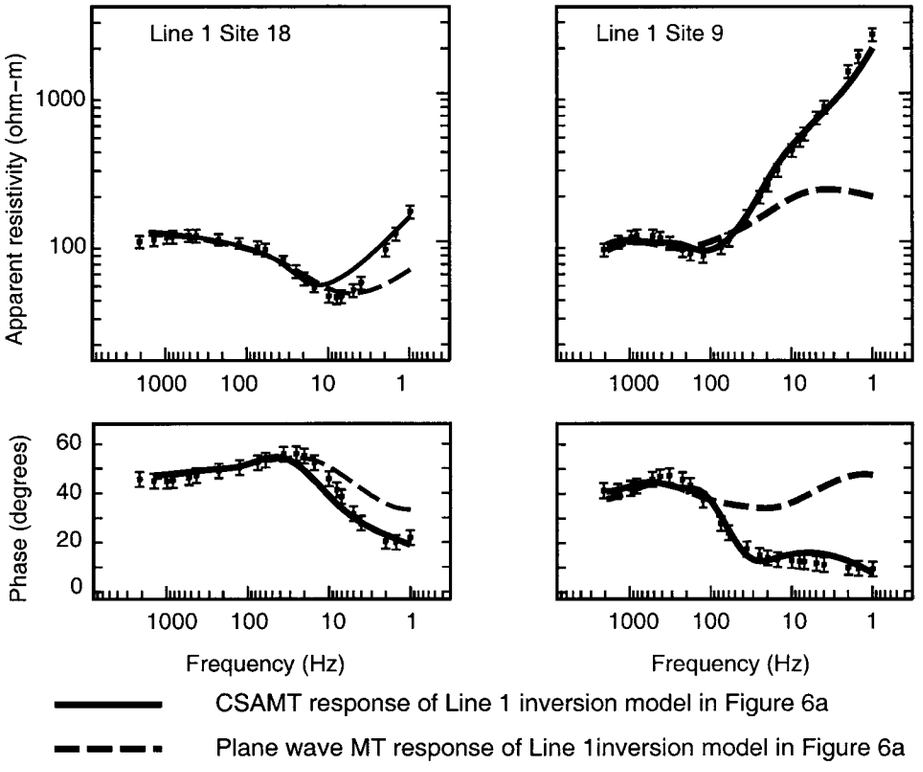

FIG. 7. CSAMT data and response of the 2-D inversion model (Figure 6a) at two sites on line 1. The plane-wave MT response of the model is shown for comparison.

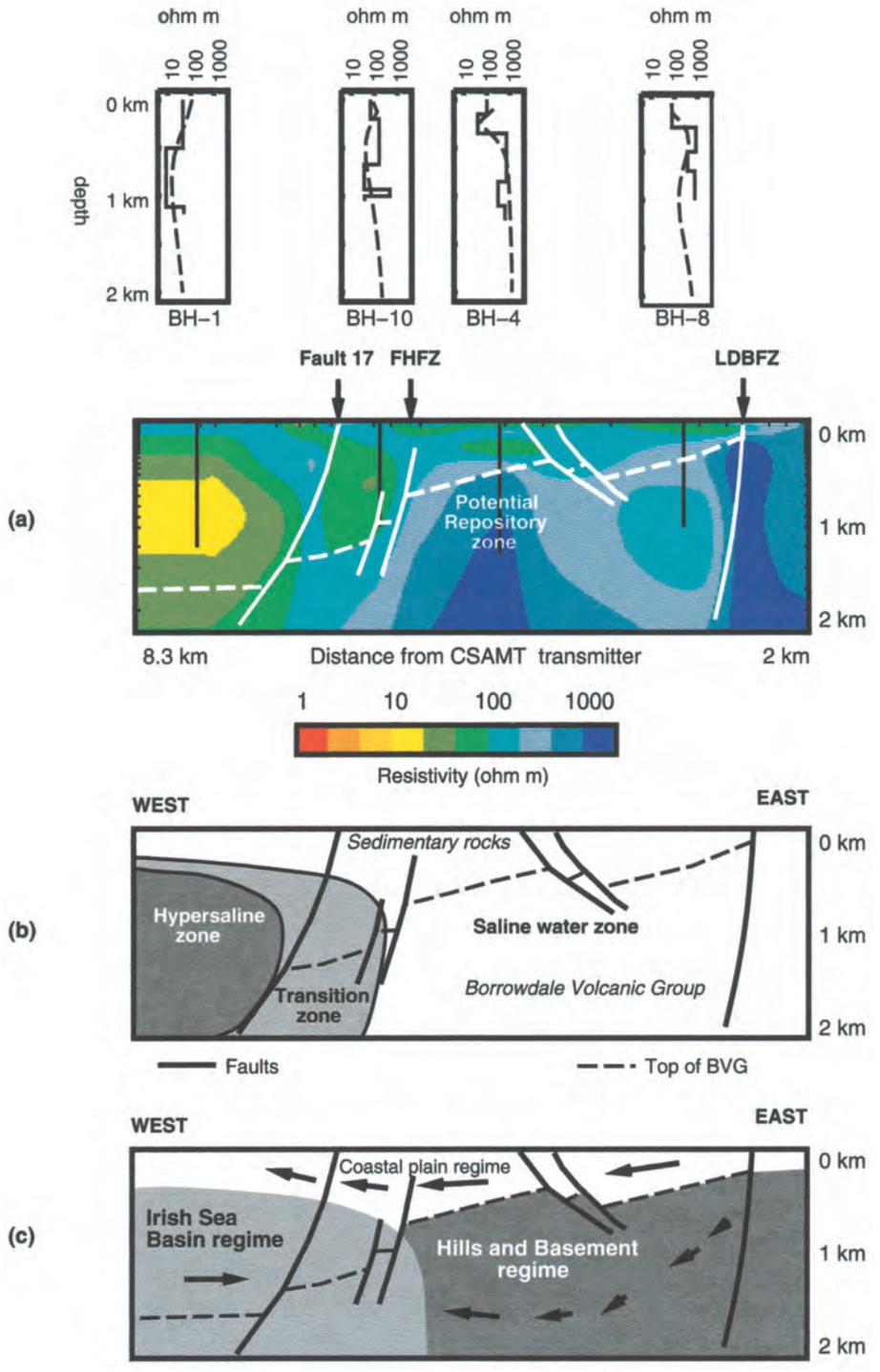

FIG. 8. (a) Resistivity model for line 1 showing comparison with well log data. (b) Geological section and interpretation. The top of the BVG is taken from Chaplow (1996). (c) Hydrogeological model of the Sellafield site from Chaplow (1996) derived from borehole measurements. Arrows denote the direction of groundwater flow.

correlates well with the top of the BVG. In the model of Chaplow (1996), this region is characterized by shallow meteoric circulation and is denoted the Coastal Plain regime.

Deeper resistive zone

The higher resistivities of this zone imply lower porosities and/or salinities than in (1) and (2). Note from Figure 8a how the top of the BVG corresponds to an increase in resistivity all the way from northeast to southwest, except in the zone of brines at the coast. This implies that the high resistivities are due in part to the change in lithology (i.e., the relatively low porosity of the BVG). Resistivities below 0.5 km at the potential waste repository are consistent with borehole salinity measurements of ~10000 mg/liter Cl (Bath et al., 1996). This region is thus inferred to have saline groundwater. The groundwater may originate through mixing of the brines derived from dissolution of salt in the sedimentary sequence with groundwater derived from precipitation on the Lake District Fells to the east. Long residence times in the BVG has caused dissolution of minerals and modified the salinity. This region is termed the Hills and Basement regime by Bath et al. (1996). Near BH-8, the inversion produces a zone where the BVG is relatively conductive, which could be due to higher porosity, possibly due to faulting within the BVG.

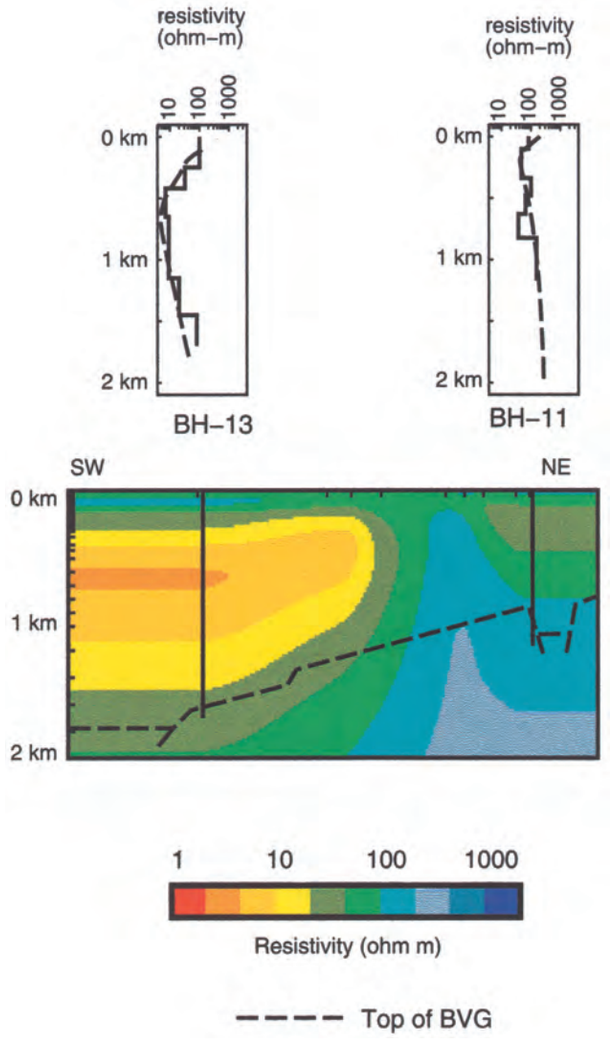

FIG. 9. Resistivity model for line 2 showing comparison with well log data. Top of BVG from Chaplow (1996).

CONCLUSIONS

In this case study, we have applied 2-D inversion to the Sellafield CSAMT data set. The differences between the results of 1-D and 2-D inversions suggest that the subsurface geology is sufficiently complex to invalidate the use of 1-D CSAMT inversions at this location. This similarity of the inversion models derived for the four profiles indicates that a 3-D analysis is probably not needed. Further justification for the validity of the 2-D inversion is provided by the reasonable agreement between the 2-D inversion models and the well log data. What proportion of the high apparent resistivity observed in Figure 4a is due to geology rather than the transmitter effect? In Figure 7, the MT response of the CSAMT inversion model in Figure 8a is shown. At site 9, the plane-wave (MT) apparent resistivity rises from ~100 ohm-m at the highest frequencies to ~200 ohm-m at the lowest frequency. In contrast, the CSAMT response rises from ~100 to ~2000 ohm-m. This shows that the rise in apparent resistivity is dominated by the transmitter effect at the potential repository site.

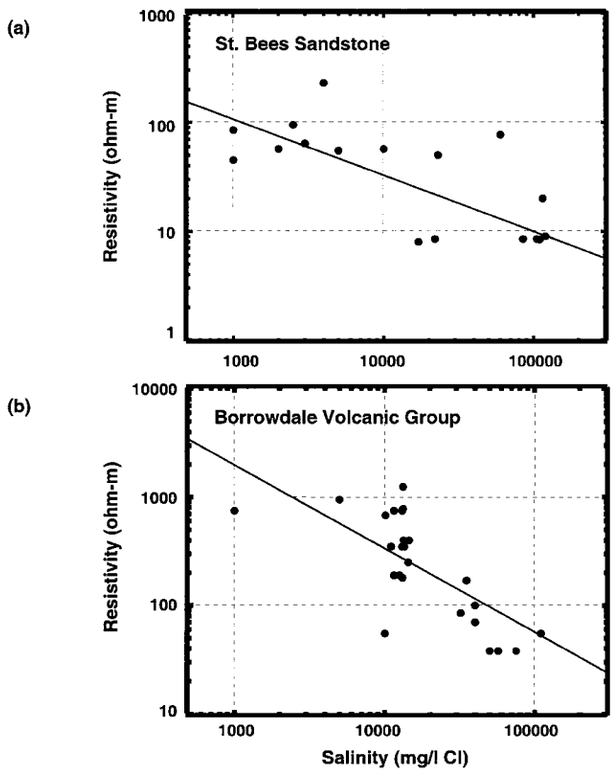

FIG. 10. Resistivity versus chloride concentration for the two principal rock types found in the near surface structure at Sellafield. Data complied from well log data and chemical analyses of groundwater samples. The straight lines represent empirical fits of resistivity (ρ) and chloride concentration ([Cl]) of the form $\rho = A[\mathrm{Cl}]^{-a}$. For the St. Bees sandstone, $a = 0.5$ and $A = 3700$ ohm-m; for the BVG, $a = 0.7$ and $A = 370\,000$ ohm-m.

These models image a significant zone of subsurface brines to the west of the potential radioactive waste repository near Sellafield. At present, the eastern limit of the zone is 1 km from the potential repository location and varies long the coast, moving offshore to the north. Hydrogeologic modeling by Heathcote et al. (1996) shows that groundwater flow in the BVG may act to keep the hypersaline zone to the west of the potential repository zone. However, variabilities in this flow over geologic time may allow it to move significantly over the lifetime of the repository.

ACKNOWLEDGMENTS

We thank United Kingdom Nirex for granting permission to publish this data. Development of the inversion code was supported by U.S. Department of Energy Grant DE-FG06-92-ER14231 to the University of Washington. This manuscript benefited greatly from reviews by Uisdean Michie, David Boerner, Torkhild Ramaussen, and an anonymous reviewer.

REFERENCES

Bartel, L. C., 1990, Results from a controlled source audio-frequency magnetotelluric survey to characterize an aquifer, *in* Ward, S. H., Ed., Geotechnical and environmental geophysics: Soc. Expl. Geophys., **2**, 219–234.

Bartel, L. C., and Jacobson, R. D., 1987, Results of a controlled-source audio frequency magnetotelluric survey at the Puhimau thermal area, Kilauea Volcano, Hawaii: Geophysics, **52**, 665–677.

Bath, A. H., McCartney, R. A., Richards, H. G., Metcalfe, R., and Crawford, M. B., 1996, Groundwater chemistry in the Sellafield area: A preliminary interpretation: Q. J. Eng. Geol., **29**, S39–57.

Boerner, D. E., and West, G. F., 1984, Efficient calculation of the electromagnetic fields of an extended source: Geophysics, **49**, 2057–2060.

Boerner, D. E., Wright, J. A., Thurlow, J. G., and Reed, L. E., 1993, Tensor CSAMT studies at the Buchans Mine in central Newfoundland: Geophysics, **58**, 12–19.

Chaplow, R., 1996, The geology and hydrogeology of Sellafield: An overview: Q. J. Eng. Geol., **29**, S1–12.

Heathcote, J. A., Jones, M. A., and Herbert, A. W., 1996, Modelling groundwater flow in the Sellafield area: Q. J. Eng. Geol., **29**, S59–81.

Lu, X., Unsworth, M. J., and Booker, J. R., 1999, Inversion of controlled source MT data: Geophys. J. Internat., **138**, 381–392.

Majer, E., Feighner, M. , Johnson, L., Daley, T. , Karageorgi, E., Lee, K. H., Kaelin, B., Williams, K., and McEvilly, T., 1996, Synthesis of borehole and surface geophysical at Yucca Mountain, Nevada and vicinity, Vol. I: Surface geophysics: Lawrence Berkeley National Laboratory Report 39319.

Michie, U., 1996, The geological framework of the Sellafield area and its relationship to hydrogeology: Q. J. Eng. Geol., **29**, S13–27.

Smith, J. T., and Booker, J. R., 1991, Rapid inversion of two- and three-dimensional magnetotelluric data: J Geophys. Res., **96**, 3905–3922.

Soonawala, N. M., Hollaway, A. L., and Tomsons, D. K., 1990, Geophysical methodology for the Canadian nuclear fuel waste management program, *in* Ward, S. H., Ed., Geotechnical and environmental geophysics: Soc. Expl. Geophys., **2**, 309–331.

Strack, K.-M., 1992, Exploration with deep transient electromagnetics: Elseiver.

Unsworth, M. J., Travis, B. J., and Chave, A. D., 1993, Electromagnetic induction by a finite dipole over a 2-D earth: Geophysics, **58**, 184–214.

Watts, M. D., 1994, Sellafield surface EM survey, electromagnetic survey factual report: NIREX Report 620.

Zonge, K. L., and Hughes, L. J., 1991, Controlled source audio-frequency magnetotellurics, *in* Nabighian, M. N., Ed., Electromagnetic methods in applied Geophysics: Soc: Expl. Geophys., **2B**, 713–908.